Extremophiles (2010) 14:213–223
DOI 10.1007/s00792-009-0300-0

ORIGINAL PAPER

Thermodynamic and kinetic stability of a large multi-domain enzyme from the hyperthermophile *Aeropyrum pernix*

Mikael Karlström · Roberta Chiaraluce · Laura Giangiacomo · Ida Helene Steen · Nils-Kåre Birkeland · Rudolf Ladenstein · Valerio Consalvi

Received: 10 September 2009 / Accepted: 21 December 2009 / Published online: 8 January 2010

Abstract The multi-domain enzyme isocitrate dehydrogenase from the hyperthermophile *Aeropyrum pernix* was studied by denaturant-induced unfolding. At pH 7.5, changes in circular dichroism ellipticity and intrinsic fluorescence showed a complex unfolding transition, whereas at pH 3.0, an apparently two-state and highly reversible unfolding occurred. Analytical ultracentrifugation revealed the dissociation from dimer to monomer at pH 3.0. The thermodynamic and kinetic stability were studied at pH 3.0 to explore the role of inter-domain interactions independently of inter-subunit interplay on the wild type and R211M, a mutant where a seven-membered inter-domain ionic network has been disrupted. The unfolding and folding transitions occurred at slightly different denaturant concentrations even after prolonged equilibration time. The difference between the folding and the unfolding profiles was decreased in the mutant R211M. The apparent Gibbs free energy decreased approximately 2 kcal/mol and the unfolding rate increased 4.3-fold in the mutant protein, corresponding to a decrease in activation free energy of unfolding of 0.86 kcal/mol. These results suggest that the inter-domain ionic network might be responsible for additional stabilization through a significant kinetic barrier in the unfolding pathway that could also explain the larger difference observed between the folding and unfolding transitions of the wild type.

Keywords Hyperthermophiles · Protein stability · Thermodynamic stability · Kinetic stability · Ionic networks · Multi-domain protein · Isocitrate dehydrogenase

Communicated by A. Driessen.

M. Karlström · R. Ladenstein
Karolinska Institutet, Center of Bioscience,
141 57 Huddinge, Sweden

R. Chiaraluce · L. Giangiacomo · V. Consalvi
Dipartimento di Scienze Biochimiche 'A Rossi Fanelli',
Università 'La Sapienza', P.le A. Moro 5, 00185 Rome, Italy

I. H. Steen · N.-K. Birkeland
Department of Biology, University of Bergen,
PO Box 7800, Jahnebakken 5, 5020 Bergen, Norway

Present Address:
M. Karlström (✉)
Department of Biochemistry and Biophysics,
The Arrhenius Laboratories, Stockholm University,
106 91 Stockholm, Sweden
e-mail: mikael.karlstrom@dbb.su.se

Introduction

Hyperthermophiles grow at or above 80°C and their proteins must be considerably more stable than those of mesophilic organisms growing at 20–50°C. Many studies have shown that hyperthermostable proteins have more ion pairs and larger ionic networks than their mesophilic counterparts (Karshikoff and Ladenstein 2001). However, the contribution of ionic interactions to protein stability has remained unclear. The investigations of the thermodynamic stability of hyperthermostable proteins are based on studies on small single-domain proteins below 25 kDa because they often exhibit a two-state reversible transition between the folded and the unfolded states (Luke et al. 2007; Privalov 1979). Thus, the Gibbs free energy difference, ΔG, between the two states can be retrieved from the equilibrium constant, K:$\Delta G = -RT \ln K$, where R is the universal gas constant and T is the temperature. In contrast, large multi-domain proteins are prone to aggregation or

irreversible unfolding, and the transition pathway often contains one or more intermediates corresponding to the discrete folding of individual domains (Jaenicke and Böhm 1998; Privalov 1982).

Studies on the kinetic stability of small hyperthermostable proteins have often revealed a significant decrease in the unfolding rate constant, k_u, compared to the values for their mesophilic counterparts, whereas the folding rate constant, k_f, appears to be similar to that of the mesophilic homologs (Cavagnero et al. 1998; Dams and Jaenicke 1999; Perl et al. 1998). Slow unfolding kinetics is equivalent to a high activation free energy barrier for unfolding, $\Delta G^{\ddagger}$. Large barriers in the protein folding landscape may prevent the folding and unfolding reactions from reaching an apparent equilibrium (Baker and Agard 1994). In such a case, the stability of the protein is under kinetic control rather than governed by a thermodynamic equilibrium (Kelch and Agard 2007).

Here, we investigate the stability of a large hyperthermostable multi-domain protein, the enzyme isocitrate dehydrogenase from *Aeropyrum pernix* (*Ap*IDH). It is functional as a dimer with a molecular mass of 47.9 kDa per subunit. *Ap*IDH is the most thermostable IDH known with an apparent melting temperature, $T_{m,app}$ of 109.9°C (Steen et al. 2001). We solved the crystal structure previously (Karlström et al. 2005). Each subunit is composed of 435 amino acid residues and consists of three domains: a large domain, a small domain, and a clasp domain which interlocks the two subunits. The large domain contains both the N- and the C-termini, whereas the small and clasp domains form the subunit interface. A preliminary investigation suggested that a seven-membered inter-domain ionic network contributes to the thermal resistance of *Ap*IDH at neutral pH (Karlström et al. 2005). In this report, the influence of a mutation in the seven-membered inter-domain ionic network will be investigated and discussed. The study aims also at contributing to the limited knowledge on thermodynamic and kinetic stability of large hyperthermostable proteins in general.

Materials and methods

Chemicals and buffers

All experiments were made using 25 mM sodium formate/formic acid pH 3.0 and 25 mM Tris/HCl pH 7.5 containing 100 μM EDTA (FLUKA) and 0.01% Tween 20 (Pharmacia) unless otherwise stated. Urea was bought from FLUKA. All buffers and solutions were prepared with ultra-high quality water (ELGA UHQ, Veolia Water Systems, High Wycombe, UK), filtered (0.22 μm) and carefully degassed.

Enzyme preparation and assay

The mutant R211M and the recombinant wt *Ap*IDH were produced in *Escherichia coli* BL21-CodonPlus (DE3)-RIL and purified with heat treatment and Red-Sepharose chromatography as previously described (Karlström et al. 2005; Steen et al. 2001). Protein concentration was determined using an absorption coefficient of $A_{280nm} = 1.288\ \text{cm}^{-1}(\text{mg/ml})^{-1}$. Enzyme activity was measured at 50°C in 25 mM Tris–HCl, pH 7.5 containing 1 mM isocitrate, 10 mM $MgCl_2$, 0.5 mM NADP, and 0.025 μg/ml enzyme in a final volume of 1 ml. The initial velocity was determined by monitoring the absorbance of NADPH formed at 340 nm on a Perkin Elmer λ 16 spectrophotometer.

Differential scanning microcalorimetric measurements

Differential scanning calorimetry (DSC) was carried out with a MicroCal MCS calorimeter controlled by the MCS OBSERVER program (MicroCal). The samples were dialyzed against the reference buffer used in the experiment (25 mM formate buffer, pH 3.0, 100 μM EDTA and 0.01% Tween 20) and degassed for 20 min prior to the calorimetric analysis. A protein concentration of 1.4 mg/ml was used. The calorimetric scans were carried out between 20 and 120°C using a scan rate of 1 K/min. A constant pressure of 2 bars was applied in order to avoid boiling at high temperatures. Each sample was scanned a second time to estimate the reversibility of the unfolding transition.

Molecular mass estimation by analytical ultracentrifugation

All experiments were conducted at 20°C on a Beckman Optima XL-A analytical ultracentrifuge equipped with absorbance optics. The protein concentration was in the range 0.2–1.0 mg/mL. Sedimentation velocity experiments were done at 40,000 rpm. Data were collected at 280 nm at a spacing of 0.005 cm with 3 averages in a continuous scan mode and were analyzed with the program Sedfit (Schuck and Rossmanith 2000). Sedimentation coefficients were corrected to $s_{20,w}$ using standard procedures. Sedimentation equilibrium experiments were performed at 16,000, 19,000 and 22,000 rpm. Data were collected at 280 nm at a spacing of 0.001 cm with 10 averages in a step-scan mode. Establishment of equilibrium was checked by comparing 8 scans up to 24 h. Data sets were edited with REEDIT (J. Lary, National Analytical Ultracentrifugation Center, Storrs, CT, USA) and fit with NONLIN (PC version provided by E. Braswell, National Analytical Ultracentrifugation Center, Storrs, CT, USA) (Johnson et al. 1981). Data from different speeds were combined for global fitting. Fits

to a single species give a Z-average molecular weight. For fits to a monomer–dimer association scheme, the monomer molecular weight was fixed at the value determined from the amino acid sequence. The experiments were performed in 20 mM Tris–HCl, pH 7.5, and in 20 mM sodium formate, pH 3.0, containing 100 μM EDTA and 0.01% Tween 20.

Spectroscopic techniques

Intrinsic fluorescence emission measurements were performed with a LS50B PerkinElmer spectrofluorimeter using 3 nm bandwidth for the excitation and 5 nm for the emission in a 1.0 cm pathlength quartz cuvette. Fluorescence emission spectra were recorded at 300–450 nm (1 nm sampling interval) at 20°C with the excitation wavelength set at 295 nm. To check for the presence of aggregated particles, light scattering intensity at 90° was measured at 20°C with both excitation and emission wavelength set at 480 nm. Far-UV (190–250 nm) and near-UV (250–320 nm) CD measurements were performed at 20°C in 0.1–0.2 cm and 1.0 cm pathlength quartz cuvettes, respectively. CD spectra were recorded on a Jasco J-720 spectropolarimeter. The results are expressed as the mean residue ellipticity [Θ] assuming a mean residue weight of 110 Dalton per amino acid residue.

Urea-induced equilibrium unfolding and folding

For unfolding, protein samples were incubated at 50 μg/ml final concentration at increasing concentrations of urea (0–8 M) in 25 mM formate pH 3.0, in 25 mM Tris–HCl pH 7.5. After 2 h, a time that was established to be sufficient to reach equilibrium since after 72-h incubation, no further changes of the IDH spectral properties were observed; intrinsic fluorescence emission and far-UV CD spectra were recorded in parallel at 20°C. For folding, protein was unfolded overnight at 20°C in 8 M urea at pH 3.0. The folding was started by 20-fold dilution of the mixture containing unfolded protein, at 20°C, into solutions of the same buffer used for unfolding containing decreasing denaturant concentrations. The final enzyme concentration was 50 μg/ml. After 2 h, intrinsic fluorescence emission and far-UV CD spectra were recorded at 20°C. All measurements were corrected for background signal of media containing the corresponding concentration of urea and repeated at least twice. The changes in intrinsic fluorescence emission spectra with increasing denaturant concentrations were monitored by the decrease of relative fluorescence intensity at 340 nm or by the changes of the averaged emission wavelength $\overline{\lambda}$, calculated according to

$$\overline{\lambda} = \sum (I_i \lambda_i) / \sum (I_i) \quad (1)$$

where λ_i and I_i are the emission wavelength and its corresponding fluorescence intensity at that wavelength, respectively (Royer et al. 1993). $\overline{\lambda}$ is an integral quantity, negligibly influenced by the noise, which reflects changes in the shape and position of the emission spectrum. The changes in far-UV CD ellipticity were monitored at 222 nm.

Urea-induced unfolding and folding kinetics

The unfolding rates of wt *Ap*IDH and the mutant R211M were determined at pH 3.0 by monitoring the rate of intrinsic fluorescence emission decrease at 340 nm (5 nm bandwidth) (excitation at 295 nm, 3 nm bandwidth) upon mixing the protein under continuous stirring into solutions containing decreasing urea concentration (from 8 to 3.75 M) at pH 3.0 and 20°C for a time ranging between 0 and 1,000–6,000 s. The recording of the unfolding time courses was possible using manual mixing methods because of the slow unfolding rates. The mixing dead time, calculated by diluting *N*-acetyl tryptophan amide under the same conditions, was always between 2 and 3 s for all the urea concentrations used. Kinetic changes in intrinsic fluorescence amplitude matched the respective static changes in the equilibrium transition at all denaturant concentrations.

Single mixing kinetic folding experiments were carried out on a Π-star 180 stopped-flow instrument equipped with a 2-μl observation cell (Applied Photophysics, Leatherhead, UK); the excitation wavelength was 280 nm, and the fluorescence emission was measured using a 320-nm cut-off glass filter. In all experiments, performed at 20°C, folding was initiated by a 11-fold dilution of the unfolded protein with the buffer. Final protein concentrations were typically 1 μM.

Data analysis

The denaturant-induced equilibrium unfolding was analyzed by fitting the data to Eq. 2 (Santoro and Bolen 1988) using the Igor Pro software package (WaveMetrics):

$$y_i = \frac{y_f + m_f[X]_i + (y_u + m_u[X]_i) \times \exp\left[\frac{(-\Delta G^{H_2O} - m_g[X]_i)}{RT}\right]}{1 + \exp\left[\frac{(-\Delta G^{H_2O} - m_g[X]_i)}{RT}\right]} \quad (2)$$

where y_i is the observed signal, y_u and y_f are the baseline intercepts for unfolded and folded protein, m_u and m_f are the baseline slopes for the unfolded and folded protein, $[X]_i$ the denaturant concentration after the ith addition, ΔG^{H_2O} the extrapolated free energy of unfolding in the absence of denaturant, m_g the slope of a $G_{unfolding}$ versus $[X]$ plot.

Kinetic analysis of the unfolding process was performed by fitting the time courses by non-linear regression analysis to a single exponential to determine the rate constant, k_u (obs, D), for unfolding at each urea concentration, D, with the program TableCurve (Systat). The unfolding rate in the absence of denaturant, k_u (H_2O), was estimated by linear extrapolation using the equation:

$$\ln k_u(\text{obs}, D) = \ln k_u(H_2O) + m_u[D] \quad (3)$$

where k_u(obs, D) is the apparent first-order rate constant for unfolding at denaturant concentration [D], k_u(H_2O) is the apparent rate constant in the absence of denaturant, and m_u describes the denaturant dependence, which is related to the change in solvent accessibility of the unfolded state (Bieri and Kiefhaber 2000; Tanford 1970).

The activation energy of unfolding, $\Delta G_u^{\ddagger}$, is related to the unfolding rate constant, k_u, by:

$$\Delta G_u^{\ddagger} = -RT \ln\left(\frac{k_u h}{k_B T}\right) \quad (4)$$

where h is the Planck constant and k_B is the Boltzmann constant (D'Amico et al. 2003). The difference in activation free energy of unfolding upon mutation, $\Delta\Delta G_u^{\ddagger}$, was calculated from the extrapolated rate constants using the following equation:

$$\Delta\Delta G_u^{\ddagger} = -RT \ln\left(\frac{k_{u,wt}}{k_{u,R211M}}\right) \quad (5)$$

where $k_{u,wt}$ and $k_{u,R211M}$ are the unfolding rate constants of the wildtype and mutant protein, respectively, extrapolated to 0 M urea concentration (Clarke et al. 1993).

Results

Enzymatic activity, reversibility, and apparent melting temperatures

The reversibility of unfolding was estimated by the recovery of fluorescence intensity at 340 nm after refolding at pH 3.0. In addition, the activity of refolded wt *Ap*IDH and R211M was measured at pH 7.5 to estimate the reversibility of the unfolding process at pH 3.0. The recovery of activity was always >95% and suggests that the refolded protein, at pH 7.5, is dimeric and that both domains are intact since each subunit contains an active site composed by residues from the large and the small domain (Karlström et al. 2005). The calorimetric scans were irreversible, presumably due to high protein concentration, and could not be used in a thermodynamic analysis. The apparent T_m values obtained at pH 3.0 were 70.6 and 67.4°C for wt *Ap*IDH and R211M, respectively, e.g. a decrease of 3.2°C upon disruption of the ionic network (data not shown).

Quaternary structure analysis by analytical ultracentrifugation

Analytical ultracentrifugation (AUC) was used to evaluate the quaternary structure of wt *Ap*IDH and R211M at pH 3.0 and 7.5. Both a velocity analysis and an equilibrium analysis were performed. The obtained $s_{20,w}$ constants 3.6 and 5.8 for wt *Ap*IDH at pH 3.0 and 7.4 correspond to a molecular weight of approximately 45 and 90 kDa in accordance with the presence of a monomer and a dimer, respectively (Fig. 1a). Sedimentation equilibrium data and the errors obtained for a fit to a single species model gave molecular weights of 46 ± 4 and 100 ± 7 kDa at pH 3.0 and 7.5, respectively, in very good agreement with the expected values for a monomer and a dimer (Fig. 1b). In the figure showing the sedimentation equilibrium, the exponential distribution of the protein along the radius is represented. At pH 3.0, the curve is less pronounced, due to the lower molecular weight of the monomer with respect to the dimer. AUC studies of R211M gave very similar results (data not shown). Taken together, the AUC experiments showed that both wt *Ap*IDH and the mutant R211M are monomeric at pH 3.0 and dimeric at pH 7.5.

Tertiary structure analysis by near-UV CD

In order to detect any tertiary structural differences of wt *Ap*IDH and the mutant R211M at pH 3.0 and 7.5, near-UV CD spectra of the two enzymes were recorded. The spectra of wt *Ap*IDH (Fig. 2a) and R211M (Fig. 2b) at pH 3.0 were nearly identical, and they both were closely similar to spectra of the corresponding dimers at pH 7.5, thus indicating that the tertiary structure of the *Ap*IDH monomers was maintained at pH 3.0 in the wild type as well as in the mutant.

Urea-induced equilibrium unfolding of wt *Ap*IDH monitored by intrinsic fluorescence

At pH 7.5, the unfolding transition of *Ap*IDH was complex in guanidinium-Cl and not complete in urea (data not shown). At pH 3.0, in the monomeric state, the protein could be completely unfolded by urea in a reversible and apparently two-state process. Fluorescence emission spectra were recorded at different denaturant concentrations to monitor the unfolding/folding transition. Both fluorescence emission intensity and the averaged fluorescence emission wavelength ($\overline{\lambda}$) were analyzed. The fluorescence emission as a function of denaturant concentration characterizes the local environment of the aromatic side chains and is

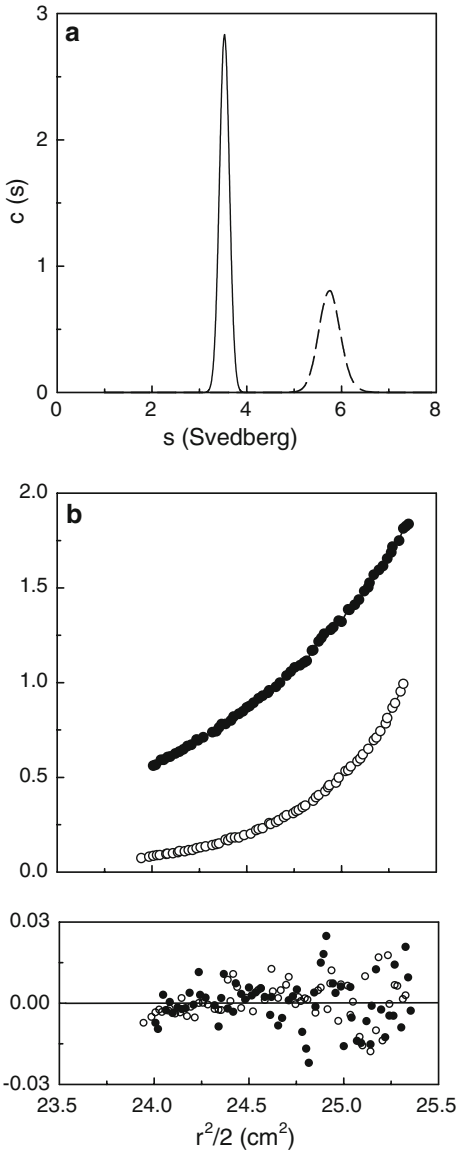

Fig. 1 Analytical ultracentrifugation of wt *Ap*IDH at pH 3.0 and 7.5. **a** Sedimentation velocity data at pH 3.0 (*continuous line*) and at pH 7.5 (*dashed line*). The $s_{20,w}$ constants 3.6 and 5.8 correspond to a molecular weight of approximately 45 and 90 kDa. **b** Sedimentation equilibrium data (*filled circles* pH 3.0, *open circles* pH 7.5) as the exponential distribution of the protein along the radius. The obtained curves correspond to 46 ± 4 and 100 ± 7 kDa at pH 3 and 7.5, in good agreement with the expected values for a monomer and a dimer, respectively. The *panel* shows the residuals

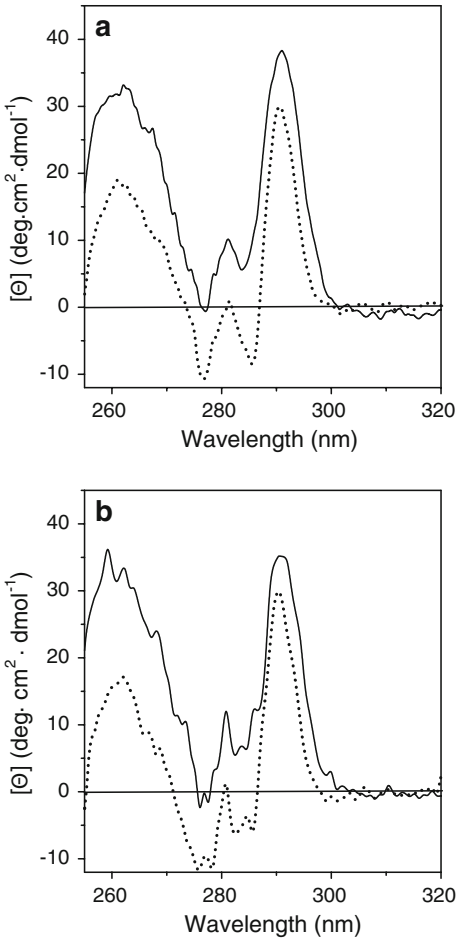

Fig. 2 Near-UV CD spectra of wt *Ap*IDH (**a**) and R211M (**b**) at pH 3.0 and 7.5. Spectra were recorded at 20°C in a 1-cm quartz cuvette after 2-h incubation at 1.1 mg/ml protein concentration at pH 7.5 (*solid line*) and at pH 3.0 (*dotted line*)

usually directly related to the population of macrostates in a two-state N ⇄ U transition (Eftink 1994).

The emission spectral changes upon unfolding of monomeric wt *Ap*IDH at pH 3.0 are shown in Fig. 3. Wt *Ap*IDH was found to have a maximum fluorescence emission wavelength at 341 nm that decreased in intensity and exhibited a red-shift to 357 nm upon incubation in 8 M urea. The $\overline{\lambda}$ value, which takes into account the global shape of the emission spectrum, displayed a maximum at 351 nm which shifted to about 365 nm above 4 M urea. The changes in the fluorescence emission intensities and in $\overline{\lambda}$ at various urea concentrations are shown in Fig. 4. Upon unfolding, the fluorescence intensity was unchanged from 0 to approximately 3.5 M urea, and the $\overline{\lambda}$ value was constant at 351 nm up to 3.8 M urea. The unfolding of the monomer occurred between 3.8 and 5 M urea, where the fluorescence intensity decreased by approximately 15% and, the $\overline{\lambda}$ value displayed a simultaneous redshift from 351 to 365 nm. In the concentration range of 5–8 M urea, both the intensity and the wavelength remained approximatively constant.

For folding, samples were incubated in 8 M urea and diluted to different urea concentrations. The intensity and maximum emission wavelengths remained nearly constant over the range 8.0–4.5 M urea. The major blue shift in the fluorescence emission spectrum occurred upon dilution to a final urea concentration between 4.5 and 1.0 M.

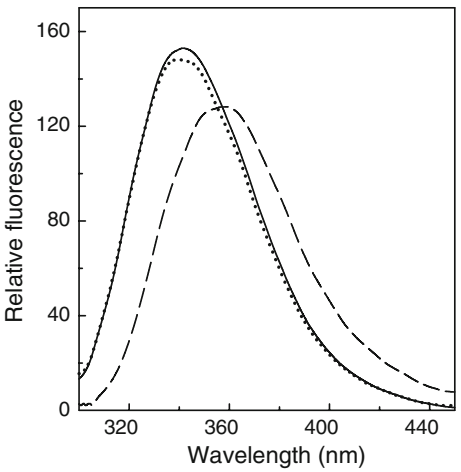

Fig. 3 Fluorescence spectra of wt *Ap*IDH at pH 3.0. Fluorescence emission spectra of the protein were recorded at 20°C after 2-h incubation of the protein at pH 3.0 in the absence (*solid line*) and in the presence of 8 M urea (*dashed line*). The *dotted line* represents the spectrum of the refolded protein. All the spectra were recorded at 50 μg/ml with the excitation wavelength set at 295 nm

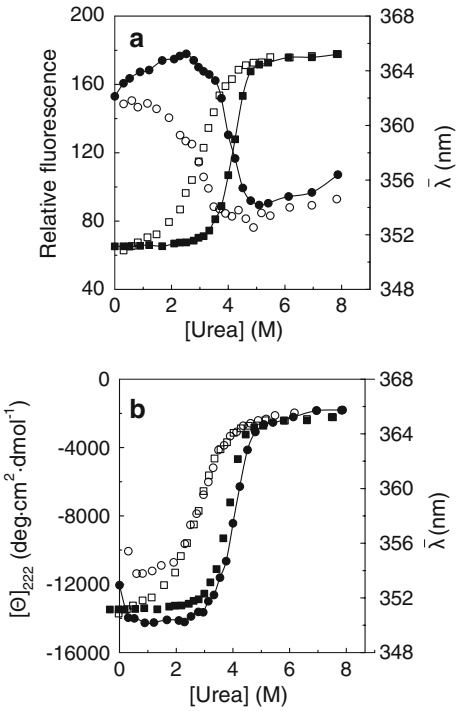

Fig. 4 Unfolding and folding transition curves of monomeric wt *Ap*IDH at pH 3.0 as monitored by circular dichroism ellipticity and fluorescence as functions of urea concentration. **a** Relative fluorescence at 340 nm (*filled circles*, *empty circles*, *left axis*); $\overline{\lambda}$ (*filled squares*, *empty squares*, *right axis*). **b** [Θ] at 222 nm (*filled circles*, *empty circles*, *left axis*); $\overline{\lambda}$ (*filled squares*, *empty squares*, *right axis*); *filled symbols* unfolding; *empty symbols* refolding. The *line* is only to guide the eye of the reader and does not represent a fit of the data

Reconstituted wt *Ap*IDH at 0.3 M urea had the same emission wavelength and a slightly lower intensity as the monomeric protein in the absence of urea (Figs. 3, 4b). The origin of the 5% lower fluorescence intensity is unclear since the protein appears to be properly folded owing to the $\overline{\lambda}$ value, its enzymatic activity when diluted at pH 7.5 and its far-UV CD spectrum. Comparing the unfolding and folding of wt *Ap*IDH, it is clear that the major unfolding event occurs at 3.5–5.0 M urea, while the folding occurs between 1.0 and 4.5 M urea, i.e. there is hysteresis between the folding and the unfolding event (Fig. 4). No significant decrease of the hysteresis could be observed after prolonged incubation up to 72 h (data not shown). The sigmoidal transition profiles of both the unfolding and folding at pH 3.0 indicated that spectral intermediate(s) are not detectable, probably because these state(s) are not consistently populated or because their spectral properties do not allow their detection.

Urea-induced equilibrium unfolding of wt *Ap*IDH monitored by far-UV CD

In order to monitor the changes of the secondary structure of monomeric wt *Ap*IDH upon unfolding and folding, far-UV CD spectra were recorded. The far-UV CD spectrum of wt *Ap*IDH at pH 3.0 was unchanged with respect to that recorded at pH 7.5 (data not shown) with a minimum in the far-UV region between 212 and 223 nm, corresponding to a similar content of secondary structure as in dimeric wt *Ap*IDH at pH 7.5. The same samples used to monitor the fluorescence emission changes during the unfolding transition were used to monitor circular dichroism ellipticity to allow a direct comparison with the fluorescence data. The unfolding and folding transitions monitored by far-UV CD (Fig. 4b) were very similar to the transitions exhibited by fluorescence (Fig. 4a). From the sigmoidal unfolding curve, it seems that wt *Ap*IDH retained most of its secondary structure up to 3.5 M urea. No intermediate state could be detected. The major unfolding transition occurred between 3.5 and 5.0 M urea, similar to the data obtained with fluorescence emission. Above 5 M urea no further changes in the CD signal were observed.

For the folding transition, the CD signals are consistent with a complete loss of the secondary structure elements over a urea concentration of 8–5 M. Over the urea concentration range of 4.5–2.0 M, the native ellipticity signal is almost completely restored. Again, the results show that the unfolding and folding transitions are separated by a significant urea concentration difference, Δ[urea] $\approx$ 1.5 M for the far-UV CD data and $\approx$1 M for the data from the fluorescence changes. In Fig. 4, it can be seen that the relative change in the CD signal could almost be superimposed on the relative change in fluorescence signal for the respective enzymes, indicating an apparent two-state process (Fersht 1999).

Urea-induced equilibrium unfolding of R211M monitored by fluorescence and far-UV CD

The unfolding/folding transitions of R211M at pH 3.0 were similar to that of wt *Ap*IDH, but the difference, Δ[urea], between folding and unfolding was only ≈0.5 M. The transition profiles of the mutant are shown in Fig. 5. Fits of the apparently two-state unfolding curves were performed, despite the observed hysteresis, in order to extract apparent conformational stabilities and to compare the value of wt *Ap*IDH with that of the mutant R211M (see Fig. 6a, b). The obtained apparent ΔG values, ΔG_{app}, for wt *Ap*IDH and the mutant are also shown in Table 1 together with the respective m values and unfolding transition midpoint values, $[urea]_{0.5}$, obtained from both $\overline{\lambda}$ data and CD-data. The fits of both far-UV CD and fluorescence data showed a decreased thermodynamic stability of the mutant R211M by approximately −2 kcal/mol compared to wt *Ap*IDH.

Determination of unfolding rate constants

Estimation of the kinetic stability of monomeric wt *Ap*IDH at pH 3.0 was obtained by measuring the rate constants for unfolding over the urea concentration range of 4.3–8.0 M following the decrease of intrinsic fluorescence emission at 340 nm. All unfolding rate data could be fitted to a single-exponential decay suggesting a simple first-order two-state reaction. The unfolding rate constants were extrapolated to zero denaturant concentration (Bieri and Kiefhaber 2000). The rate constants obtained were 1.95 (±0.10) × 10^{-7} s^{-1} for monomeric wt *Ap*IDH (Fig. 7a), corresponding to a half-life of about 41 days and 8.36 (±0.20) × 10^{-7} s^{-1} for R211M (Fig. 7b), corresponding to 9.6 days. Thus, the kinetic stability of R211M was decreased 4.3-fold compared to wt *Ap*IDH. The difference in activation free energy of unfolding, $\Delta\Delta G^{\ddagger}_{u}$, between wt *Ap*IDH and R211M calculated according to Eq. 5 was 0.86 ± 0.06 kcal/mol.

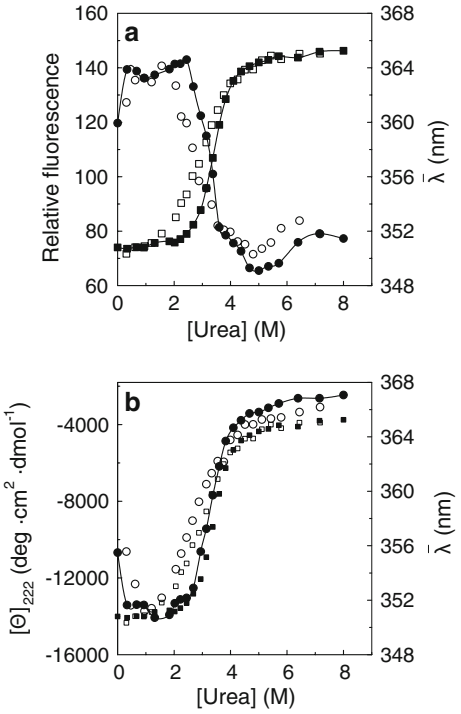

Fig. 5 Unfolding and folding transition curves of monomeric mutant R211M *Ap*IDH at pH 3.0 as monitored by circular dichroism ellipticity and fluorescence. **a** Relative fluorescence at 340 nm (*filled circles*, *empty circles*, *left axis*); intensity-averaged emission wavelength $\overline{\lambda}$ (*filled squares*, *empty squares*, *right axis*). **b** [Θ] at 222 nm (*filled circles*, *empty circles*, *left axis*); intensity-averaged emission wavelength $\overline{\lambda}$ (*filled squares*, *empty squares*, *right axis*). The *solid lines* through the unfolding data points (*filled symbols*) have the purpose to guide the eye of the reader and do not represent the fitting of the data. Reversibility points are indicated by *empty symbols*

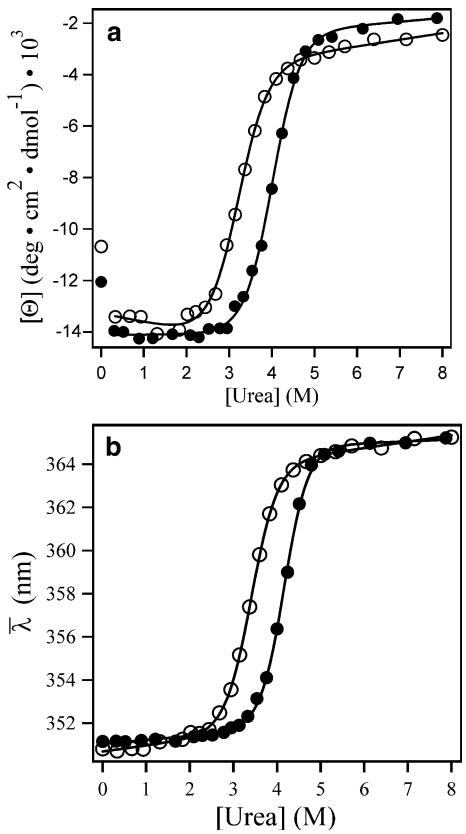

Fig. 6 Urea-induced spectral changes of wt (*filled circles*) and R211M (*empty circles*) *Ap*IDH at pH 3.0. Spectral changes are reported as **a** [Θ] at 222 nm and **b** fluorescence intensity-averaged emission wavelength $\overline{\lambda}$ calculated according to Eq. 1. All the spectra were recorded at 20°C after 2-h incubation at the indicated urea concentrations at 50 μg/mL protein concentration. Non-linear curve fitting of the unfolding data was performed using Eq. 2

Table 1 Thermodynamic and kinetic parameters for the unfolding of wt *Ap*IDH and the mutant R211M calculated from data obtained by using circular dichroism ellipticity at 222 nm, [Θ], and intensity-averaged emission wavelength, $\overline{\lambda}$

*Ap*IDH	ΔG_{app}, [Θ] (kcal/mol) [kcal/mol M^{-1}]	ΔG_{app}, $\overline{\lambda}$ (kcal/mol) [kcal/mol M^{-1}]	$[urea]_{0.5}$ [Θ]/$\overline{\lambda}$ (M)	k_u (s^{-1})	$t_{0.5}$ at 0 M urea (days)
wt	7.30 [$m = 1.82$]	9.06 [$m = 2.18$]	4.01/4.16	1.95×10^{-7}	41
R211M	5.42 [$m = 1.70$]	6.75 [$m = 1.98$]	3.19/3.41	8.36×10^{-7}	9.6

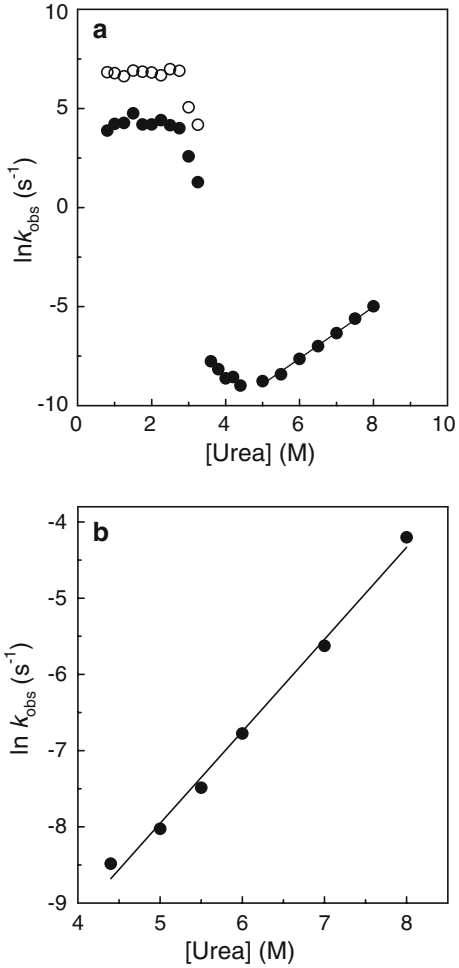

Fig. 7 **a** Unfolding and refolding kinetics of wt *Ap*IDH at pH 3.0. The *continuous line* is the fitting of the apparently linear region of the unfolding limb of the Chevron plot yielding the estimated $k_u = 1.95 \times 10^{-7}$ s^{-1}. *Empty* and *filled symbols* represent the fast and the slow refolding phase, respectively. **b** Unfolding kinetics of R211M *Ap*IDH at pH 3.0. The *continuous line* is the fitting of the unfolding data using Eq. 3 yielding the estimated $k_u = 8.36 \times 10^{-7}$ s^{-1}

The unfolding rate constants obtained under denaturing conditions corresponded to half-lives of less than 1 h, and no significant difference could be observed after a prolonged incubation time of 72 h. Thus, an incubation time of 2 h was considered as enough for the equilibrium unfolding experiments. Equilibration times longer than 72 h were not considered because of the tendency of urea solutions to form cyanate at pH values above 2 (Dirnhuber and Schutz 1948; Hagel et al. 1971), which can react with and modify proteins (Stark 1965).

Determination of folding rate constants

The folding process of wt *Ap*IDH was complex. It was significantly faster than the unfolding process and could not be described by a simple two-state event. The fluorescence signals obtained at the end of the stopped-flow mixing were best fitted to the sum of two single-exponential rate constants corresponding to two refolding phases and are shown in the chevron plot in Fig. 7a. The complex dependence of the folding rate constants upon denaturant concentrations suggests that intermediate(s) are probably formed and that kinetic traps may be present in the folding pathway. Under these circumstances, the folding limb of the chevron plot is unreliable, and the rate constants cannot be extrapolated to 0 M urea concentration (Maxwell et al. 2005). Interestingly, the $[urea]_{0.5}$ value determined by unfolding equilibrium, 4.16 M (Table 1), is closely similar to the urea concentration corresponding to the starting point of the folding limb of the chevron plot (Fig. 7).

Discussion

In this paper, studies of the thermodynamic and kinetic stability of wt *Ap*IDH and the mutant R211M, which interrupts a seven-membered ionic network, is described. At pH 3.0, the protein could be completely unfolded by urea in an apparent two-state process. Analytical ultracentrifugation demonstrated that *Ap*IDH is monomeric at pH 3.0 and dimeric at pH 7.5; thus, at pH 3.0 the intrinsic stability of the polypeptide chain could be studied independently of its subunit association state. Many proteins are completely or partially unfolded at pH 3.0 due to the repulsive forces between protonated groups (Goto et al. 1990; Privalov 1979). In the case of *Ap*IDH, far- and near-UV CD spectra indicated, however, that at pH 3.0 the secondary and tertiary structures were maintained and that the monomer is stable in solution. We therefore decided to investigate the reversible unfolding of the monomeric form of *Ap*IDH at pH 3.0. The

reversibility of unfolding at pH 3.0 was estimated by the regain of fluorescence intensity at 340 nm and by the recovery of the catalytic activity at pH 7.5 of the protein refolded at pH 3.0. The high reversibility (higher than 95%), which is uncommon for multi-domain proteins, enabled us to perform equilibrium unfolding studies. However, the unfolding and folding transitions of *Ap*IDH, as monitored by fluorescence and CD occurred at different denaturant concentrations. Apparently, both the forward and reverse reactions could proceed spontaneously, but the folded and unfolded states appeared not to be in equilibrium at the intermediate denaturant concentrations of the transition region. A possible explanation is that large energy barriers are present in the protein folding landscape, imposing additional kinetic stabilization (Baker and Agard 1994; Chan and Dill 1993) as reported for several oligomeric proteins (Baskakov et al. 2004; Benitez-Cardoza et al. 2001; Forrer et al. 2004; Galani et al. 2002; Lai et al. 1997; Miller et al. 1998; Perrett et al. 1999; Ruan et al. 2001; Sinclair et al. 1994; Souillac et al. 2002). If this would be the case, the time to reach equilibrium could be very long (i.e. several weeks; Rumfeldt et al. 2006). The situation is different in most single-domain proteins which exhibit reversible unfolding, where the native state is in equilibrium with the unfolded state at different denaturant concentrations, implying that the kinetic barriers between the folded and unfolded states are easy to overcome (Dill 1993; Lai et al. 1997).

The unfolding rate constant, k_u, and the corresponding half-life demonstrated that the unfolding of monomeric *Ap*IDH at 20°C is a slow process ($t_{0.5} = 41$ days) and suggested that the folded and unfolded states indeed may be separated by a high activation free energy barrier. In addition, the refolding kinetics of wt *Ap*IDH were complex and suggested the presence of intermediates and kinetic traps in the folding landscape that might be related to the observed difference between the unfolding and refolding profiles.

This difference was reduced in the mutant R211M and suggested that Arg 211 might have a role in kinetic stabilization of *Ap*IDH. The unfolding rate increased 4.3-fold, corresponding to a decrease in the activation free energy of unfolding of −0.86 kcal/mol which showed that the ionic network under study indeed influence the kinetic stability of *Ap*IDH at pH 3.0. In addition, the ΔG_{app} value for R211M was decreased by approximately −2 kcal/mol suggesting that the ionic network also have an impact on the thermodynamic stability.

The role of electrostatic interactions for the extreme stability of proteins from hyperthermophiles has been vigorously discussed in recent years (Karshikoff and Ladenstein 2001). However, investigations of their contribution by the removal or introduction of ionic interactions using site-directed mutagenesis have given contradicting results. In some studies, these substitutions had no effect on the resistance of the proteins against thermal inactivation or denaturation (Lebbink et al. 1998; Tomschy et al. 1994). In other cases, a significant change of the melting temperature, T_m, has been observed (Perl et al. 2000; Vetriani et al. 1998). Unfortunately, the extent of the contribution by electrostatic interactions to the thermodynamic stability of proteins from hyperthermophiles has remained unclear because of the difficulties in obtaining thermodynamic data based on unfolding-folding equilibria.

Arg 211 has a central position in the inter-domain ionic network of *Ap*IDH. Except for Arg 211, the network consists of Lys 255, Arg 215, Glu 218, and Glu 214 from the small domain and Asp 130 and Asp 334 from the large domain (Karlström 2005). In addition, Arg 211 is involved in aromatic π-interactions with Tyr 132 and Phe 207. R211M interrupts the integrity of this ionic network. However, it cannot be excluded that the introduced methionine may destabilize the protein additionally by the introduction of a hydrophobic side-chain at the protein surface and steric alteration. At pH 7.5, the apparent melting temperature of R211M was decreased by 11.3°C compared to the wildtype, suggesting an important role of the ionic network for the stability (Karlström et al. 2005). At pH 3.0, the apparent melting temperature of the monomer was decreased by about 40°C, but the difference between R211M and wt *Ap*IDH was still 3.2°C. The large decrease of the melting temperature at pH 3.0 was expected since, at low pH, protonation of the ionizable groups results in an increased number of repulsive positive charges and a decreased number of attractive electrostatic interactions, i.e. a decreased overall stability (Cavagnero et al. 1995). The pH-dependence of each ionizable group is described by its individual pK_a value which determines the preferred protonation state at a certain pH. In an NMR study of 24 proteins, Forsyth et al. (2002) found a mean pK_a of 3.4 (±1.0) for Asp and 4.1 (±0.8) for Glu with several p*K*s below 2.0. Other studies report pK_a values for Asp and Glu between 0.5 and 9.9 (Anderson et al. 1990; Giletto and Pace 1999; Laurents et al. 2003; Qin et al. 1996; Thurlkill et al. 2006). Thus, at pH 3.0, some of the negatively charged residues might be protonated, whereas some will stay ionized depending on their individual pK_a. The propensity to stay ionized is in particular dependent on the involvement in ionic networks since charge-charge interactions are the primary perturbant of the intrinsic p*K*s of ionizable groups on the protein surface (Laurents et al. 2003).

The decreased difference in melting temperature between wt *Ap*IDH and the mutant R211M observed at pH 3.0 is therefore most likely caused by a size reduction of the ionic network due to protonation of some of the negatively charged residues. The difference of 3.2°C at pH 3.0 indicates that some residues are still ionized, and part of the ionic network is maintained.

The results obtained from the thermodynamic and kinetic analysis of wt *Ap*IDH and the R211M mutant support that some of the interactions of the ionic network in wt *Ap*IDH are maintained at pH 3.0.

Conclusion

*Ap*IDH and the ionic network mutant R211M were found to be stable monomers at pH 3.0 and exhibited highly reversible unfolding transitions. The apparent melting temperature $T_{m,app}$ of R211M was decreased by 3.2°C, and the apparent free energy of stabilization, ΔG_{app}, was about 2 kcal/mol lower compared to wt *Ap*IDH. The decrease of R211M kinetic stability was remarkable considering the low pH and corresponded to a 4.3-fold increase of k_u and −0.86 kcal/mol for the activation free energy of unfolding. Presumably, the differences in thermodynamic and kinetic stability between wt *Ap*IDH and R211M are even larger at pH 7.5. The general picture which emerges is that inter-domain ionic networks in large proteins from hyperthermophiles may not only contribute to the thermodynamic stability but are also able to impose additional stabilization through a significant kinetic barrier in the unfolding pathway.

Acknowledgments We would like to thank Marit Madsen for providing us with pure protein and Stefano Gianni for critical reading of the manuscript.

References

Anderson DE, Becktel WJ, Dahlquist FW (1990) pH-induced denaturation of proteins: a single salt bridge contributes 3–5 kcal/mol to the free energy of folding of T4 lysozyme. Biochemistry 29:2403–2408

Baker D, Agard DA (1994) Kinetics versus thermodynamics in protein folding. Biochemistry 33:7505–7509

Baskakov IV, Legname G, Gryczynski Z, Prusiner SB (2004) The peculiar nature of unfolding of the human prion protein. Protein Sci 13:586–595

Benitez-Cardoza CG, Rojo-Dominguez A, Hernandez-Arana A (2001) Temperature-induced denaturation and renaturation of triosephosphate isomerase from *Saccharomyces cerevisiae*: evidence of dimerization coupled to refolding of the thermally unfolded protein. Biochemistry 40:9049–9058

Bieri O, Kiefhaber T (2000) Kinetic models in protein folding. In: Pain RH (ed) Mechanisms of protein folding, 2nd edn. Oxford University Press, Oxford

Cavagnero S, Zhou ZH, Adams MW, Chan SI (1995) Response of rubredoxin from *Pyrococcus furiosus* to environmental changes: implications for the origin of hyperthermostability. Biochemistry 34:9865–9873

Cavagnero S, Debe DA, Zhou ZH, Adams MW, Chan SI (1998) Kinetic role of electrostatic interactions in the unfolding of hyperthermophilic and mesophilic rubredoxins. Biochemistry 37:3369–3376

Chan HS, Dill KA (1993) Energy landscapes and the collapse dynamics of homopolymers. J Chem Phys 99:2116–2127

Clarke J, Hounslow AM, Bycroft M, Fersht AR (1993) Local breathing and global unfolding in hydrogen exchange of barnase and its relationship to protein folding pathways. Proc Natl Acad Sci USA 90:9837–9841

D'Amico S, Marx J-C, Gerday C, Feller G (2003) Activity-stability relationships in extremophilic enzymes. J Biol Chem 278:7891–7896

Dams T, Jaenicke R (1999) Stability and folding of dihydrofolate reductase from the hyperthermophilic bacterium *Thermotoga maritima*. Biochemistry 38:9169–9178

Dill KA (1993) Folding proteins: finding a needle in a haystack. Curr Opin Struct Biol 3:99–103

Dirnhuber P, Schutz F (1948) The isomeric transformation of urea into ammonium cyanate in aqueous solutions. Biochem J 42:628–632

Eftink MR (1994) The use of fluorescence methods to monitor unfolding transitions in proteins. Biophys J 66:482–501

Fersht A (1999) Structure and mechanism in protein science. W. H. Freeman and Company, New York

Forrer P, Chang C, Ott D, Wlodawer A, Pluckthun A (2004) Kinetic stability and crystal structure of the viral capsid protein SHP. J Mol Biol 344:179–193

Forsyth WR, Antosiewicz JM, Robertson AD (2002) Empirical relationships between protein structure and carboxyl pKa values in proteins. Proteins 48:388–403

Galani D, Fersht AR, Perrett S (2002) Folding of the yeast prion protein Ure2: kinetic evidence for folding and unfolding intermediates. J Mol Biol 315:213–227

Giletto A, Pace CN (1999) Buried, charged, non-ion-paired aspartic acid 76 contributes favorably to the conformational stability of ribonuclease T1. Biochemistry 38:13379–13384

Goto Y, Calciano LJ, Fink AL (1990) Acid-induced folding of proteins. Proc Natl Acad Sci USA 87:573–577

Hagel P, Gerding JJ, Fieggen W, Bloemendal H (1971) Cyanate formation in solutions of urea. I. Calculation of cyanate concentrations at different temperature and pH. Biochim Biophys Acta 243:366–373

Jaenicke R, Böhm G (1998) The stability of proteins in extreme environments. Curr Opin Struct Biol 8:738–748

Johnson ML, Correia JJ, Yphantis DA, Halvorson HR (1981) Analysis of data from the analytical ultracentrifuge by nonlinear least-squares techniques. Biophys J 36:575–588

Karlström M, Stokke R, Steen IH, Birkeland NK, Ladenstein R (2005) Isocitrate dehydrogenase from the hyperthermophile *Aeropyrum pernix*: X-ray structure analysis of a ternary enzyme-substrate complex and thermal stability. J Mol Biol 345:559–577

Karshikoff A, Ladenstein R (2001) Ion pairs and the thermotolerance of proteins from hyperthermophiles: a "traffic rule" for hot roads. Trends Biochem Sci 26:550–556

Kelch BA, Agard DA (2007) Mesophile versus thermophile: insights into the structural mechanisms of kinetic stability. J Mol Biol 370:784–795

Lai Z, McCulloch J, Lashuel HA, Kelly JW (1997) Guanidine hydrochloride-induced denaturation and refolding of transthyretin exhibits a marked hysteresis: equilibria with high kinetic barriers. Biochemistry 36:10230–10239

Laurents DV, Huyghues-Despointes BM, Bruix M, Thurlkill RL, Schell D, Newsom S, Grimsley GR, Shaw KL, Trevino S, Rico M, Briggs JM, Antosiewicz JM, Scholtz JM, Pace CN (2003) Charge-charge interactions are key determinants of the pK values of ionizable groups in ribonuclease Sa (pI = 3.5) and a basic variant (pI = 10.2). J Mol Biol 325:1077–1092

Lebbink JH, Knapp S, van der Oost J, Rice D, Ladenstein R, de Vos WM (1998) Engineering activity and stability of *Thermotoga maritima* glutamate dehydrogenase. I. Introduction of a six-residue ion-pair network in the hinge region. J Mol Biol 280:287–296

Luke KA, Higgins CL, Wittung-Stafshede P (2007) Thermodynamic stability and folding of proteins from hyperthermophilic organisms. FEBS J 274:4023–4033

Maxwell KL, Wildes D, Zarrine-Afsar A, De Los Rios MA, Brown AG, Friel CT, Hedberg L, Horng JC, Bona D, Miller EJ, Vallee-Belisle A, Main ER, Bemporad F, Qiu L, Teilum K, Vu ND, Edwards AM, Ruczinski I, Poulsen FM, Kragelund BB, Michnick SW, Chiti F, Bai Y, Hagen SJ, Serrano L, Oliveberg M, Raleigh DP, Wittung-Stafshede P, Radford SE, Jackson SE, Sosnick TR, Marqusee S, Davidson AR, Plaxco KW (2005) Protein folding: defining a "standard" set of experimental conditions and a preliminary kinetic data set of two-state proteins. Protein Sci 14:602–616

Miller S, Schuler B, Seckler R (1998) A reversibly unfolding fragment of P22 tailspike protein with native structure: the isolated beta-helix domain. Biochemistry 37:9160–9168

Perl D, Welker C, Schindler T, Schroder K, Marahiel MA, Jaenicke R, Schmid FX (1998) Conservation of rapid two-state folding in mesophilic, thermophilic and hyperthermophilic cold shock proteins. Nat Struct Biol 5:229–235

Perl D, Mueller U, Heinemann U, Schmid FX (2000) Two exposed amino acid residues confer thermostability on a cold shock protein. Nat Struct Biol 7:380–383

Perrett S, Freeman SJ, Butler PJ, Fersht AR (1999) Equilibrium folding properties of the yeast prion protein determinant Ure2. J Mol Biol 290:331–345

Privalov PL (1979) Stability of proteins: small globular proteins. Adv Protein Chem 33:167–241

Privalov PL (1982) Stability of proteins. Proteins which do not present a single cooperative system. Adv Protein Chem 35:1–104

Qin J, Clore GM, Gronenborn AM (1996) Ionization equilibria for side-chain carboxyl groups in oxidized and reduced human thioredoxin and in the complex with its target peptide from the transcription factor NF kappa B. Biochemistry 35:7–13

Royer CA, Mann CJ, Matthews CR (1993) Resolution of the fluorescence equilibrium unfolding profile of trp aporepressor using single tryptophan mutants. Protein Sci 2:1844–1852

Ruan Q, Ruan K, Balny C, Glaser M, Mantulin WW (2001) Protein folding pathways of adenylate kinase from *E. coli*: hydrostatic pressure and stopped-flow studies. Biochemistry 40:14706–14714

Rumfeldt JA, Stathopulos PB, Chakrabarrty A, Lepock JR, Meiering EM (2006) Mechanism and thermodynamics of guanidinium chloride-induced denaturation of ALS-associated mutant Cu, Zn superoxide dismutases. J Mol Biol 355:106–123

Santoro MM, Bolen DW (1988) Unfolding free energy changes determined by the linear extrapolation method. 1. Unfolding of phenylmethanesulfonyl alpha-chymotrypsin using different denaturants. Biochemistry 27:8063–8068

Schuck P, Rossmanith P (2000) Determination of the sedimentation coefficient distribution by least-squares boundary modeling. Biopolymers 54:328–341

Sinclair JF, Ziegler MM, Baldwin TO (1994) Kinetic partitioning during protein folding yields multiple native states. Nat Struct Biol 1:320–326

Souillac PO, Uversky VN, Millett IS, Khurana R, Doniach S, Fink AL (2002) Effect of association state and conformational stability on the kinetics of immunoglobulin light chain amyloid fibril formation at physiological pH. J Biol Chem 277:12657–12665

Stark GR (1965) Reactions of cyanate with functional groups of proteins. II. Formation, decomposition, and properties of N-carbamylimidazole. Biochemistry 4:588–595

Steen IH, Madern D, Karlstrom M, Lien T, Ladenstein R, Birkeland NK (2001) Comparison of isocitrate dehydrogenase from three hyperthermophiles reveals differences in thermostability, cofactor specificity, oligomeric state, and phylogenetic affiliation. J Biol Chem 276:43924–43931

Tanford C (1970) Protein denaturation. C. Theoretical models for the mechanism of denaturation. Adv Protein Chem 24:1–95

Thurlkill RL, Grimsley GR, Scholtz JM, Pace CN (2006) Hydrogen bonding markedly reduces the pK of buried carboxyl groups in proteins. J Mol Biol 362:594–604

Tomschy A, Bohm G, Jaenicke R (1994) The effect of ion pairs on the thermal stability of D-glyceraldehyde 3-phosphate dehydrogenase from the hyperthermophilic bacterium *Thermotoga maritima*. Protein Eng 7:1471–1478

Vetriani C, Maeder DL, Tolliday N, Yip KS, Stillman TJ, Britton KL, Rice DW, Klump HH, Robb FT (1998) Protein thermostability above 100 degreesC: a key role for ionic interactions. Proc Natl Acad Sci USA 95:12300–12305